HAIT Journal of Science and Engineering B, Volume 2, Issues 1-2, pp. 242-253

Water oxygenation in an experimental aerator with different air/water interaction patterns

Semyon P. Levitsky[1], Leonid N. Grinis[1], Jehuda Haddad[1], and Michael P. Levitsky[2,*]

[1] *Negev Academic College of Engineering, Beer-Sheva, 84100, Israel,*
[2] *Institute for Industrial Mathematics, Beer-Sheva, 84311, Israel*
[*] *Corresponding author: levitsky@iimath.com*

Received 15 July 2004, revised 22 September 2004, accepted 28 October 2004

Abstract

A device for water saturation by gas using enhanced air-water interaction is studied experimentally. The flow of gas and water in the device is organized in a way providing efficient gas dispersion into fine bubbles at relatively low gas and liquid supply pressures. It permits water oxygenation to be improved and the aeration expenses to be reduced as compared with existing aerators. The setup for experimental study of the device and the measurement procedure are described. The data obtained confirm efficiency of the proposed aerator for water oxygenation.

PACS: 89.60.-k, 89.20.Bb, 47.85.-g, 47.62.+q, 47.60.+I, 47.55.-t

1 Introduction

The activated sludge process (ASP) has gained wide-spread acceptance in biological wastewater treatment. The role of aeration in ASP is to provide oxygen to microorganisms as they assimilate the organic carbon compounds and digest a portion of them to carbon dioxide and water, sulfate and nitrate compounds. The water aeration equipment used in this process consumes as much as 60-80% of total power requirements in modern wastewater treatment plants [1]. For instance, in wastewater facilities blowers for aeration of

activated sludge account for half the electricity, and pumping for 15% [2]. The total electricity consumed in water and wastewater treatment facilities in the USA amounts to 3%. As power costs increase, more energy-efficient systems such as fine-bubble, full-floor coverage systems and jet injectors replace the older and less efficient aeration systems such as coarse-bubble, spiral-roll diffusers, etc.

Many technologies are in use at present for aeration in the ASP. The most commonly employed are coarse or fine bubble diffusion, surface aerators and brush aerators (propeller aspirator pumps and paddlewheel aerators), Ventury aeration systems.

Propeller aspirator pumps are good aerators in ponds, but are intended for a sufficiently deep water (1-5 m). When used in shallow ponds they have a tendency to scour hollows where the water stream collides with the pond bottom, so care must be taken when they are installed to avoid this problem [3]. The paddlewheel usually works well in a standard pond with surface area of 1000 m^2 and a maximum depth of 1.5-2 m [3]. Its efficiency is explained by its ability to destratify a pond rapidly through strong water circulation as well as by good aeration resulting from spraying water into air and dragging air into water at large air/water interface.

A widespread aeration technology is based on the oxygen dissolution in wastewater from air bubbles. As the bubbles move through the water, oxygen diffuses into liquid by transfer across the bubble surface. In coarse diffuser systems the air mass pushes out through large orifices because they are less prone to plug. Originally, most diffused air systems used fine bubbles with small diameters created by porous type media such as ceramic plates. The small bubbles will contain the same volume of air in a greater number of bubbles. Fine bubbles are much more efficient at air transfer because they create a larger transfer surface area per unit of added air. For instance, coarse bubble diffusion is characterized usually by oxygen transfer efficiency (OTE) of about 0.75% per foot of pond depth, while the fine bubble systems may have OTE of up to 2% per foot [4].

Different effects of air flow rate on oxygen transfer efficiency have been reported. When brush aerators are used, the oxygen transfer rate can be increased with supporting bubble aeration (according to [5], up to 50%). In bubble-diffused aeration systems the coefficient of oxygen transfer K increases with the airflow rate and water temperature, but decreases with the water depth [6, 7]. At the same time, reducing the air flow velocity per fine pore diffuser (40 μ and 140 μ pore diameter diffusers were used [8]) significantly increased K. A decrease in orifice diameter from 140 μ to 40 μ had no effect on K (the mean bubble size produced by 40 μ and 140 μ

diffusers was 4.0 mm and 4.2 mm, respectively [8]). In attempt to improve the performance of diffused aeration new methods were implemented that would promote instabilities inside the air-water-fiber medium [9]. By implementing an air cycling method, it is possible to make more efficient use of the air to mitigate fouling and further reduce life cycle costs.

The important variable that affects oxygen transfer efficiency is water quality, which includes the presence and concentration of surfactants such as detergents, dissolved solids, and possibly suspended solids. Changes in bubble shape and size occur when the water is contaminated with surfactants. Studies of this effect showed that OTE decreases in the presence of surfactants [10, 11]. By altering the surface tension, they often cause fine bubbles to coalesce into fewer larger bubbles. In addition, a thin film of detergent molecules between the air bubble and the wastewater can act as a barrier, increasing resistance to oxygen transfer.

More effective for the aeration process is the technology using Ventury-type jet ejectors connected to various nozzles. Studies conducted by Environmental Dynamics Inc., USA [3], have found that the use of ejector technology in aeration raises its efficiency in wastewater up to 3 times. However, according to experimental data, the gas/liquid mass flow ratio in that case is in the 0.5-0.55 range, which raises the cost of the aeration process.

Unfortunately, the phenomena underlying aeration processes have not yet been fully understood. The oxygen transfer rate from gas to liquid phase depends on such factors as aeration method, power input intensity, mixing intensity or turbulence, temperature, test facility geometry, and physicochemical properties of the liquid [12, 13]. Therefore, the development of new devices for air/water interaction providing for high OTE at low operation costs and as small as possible air supply pressures is a major present issue.

2 Experimental setup

The design of the experimental setup is shown in Fig. 1. It is made so as to enable the testing of different arrangements for water/air interaction, in particular, by altering the positions for gas/liquid supply. The setup comprises the body 1 containing bushing 2. The bushing channel is shaped as a Ventury tube and contains the convergent unit 3, the throat 4 with 14 mm diameter, and the diffuser 5. The convergent and divergent sections angles are 45° and 10°, respectively. The body and the bushing are made of Plexiglas for visual observation of the air/water interaction process. The

diffuser outlet is located in the recess 6 of the body. The nozzle 7 is installed into the bushing 2 locked against the end for supply of the water to be saturated by air oxygen. The nozzle is fixed in the bushing by the adapter 8.

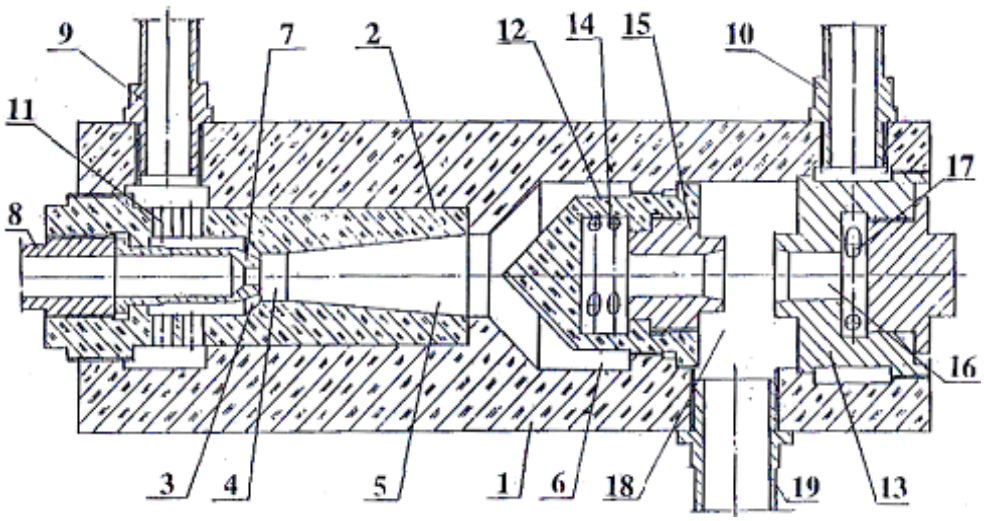

Figure 1: Design of the experimental setup.

The air is supplied through two nosepieces 9 and 10 with inner diameters of 14 mm. The inner chamber of the bushing 2 is connected to the air supply reservoir by the ducts 11.

To realize another arrangement for air/water interaction, two swirl chambers 12 and 13 are additionally installed in the body. The swirl chamber 12, also made of Plexiglas, has tangential ducts 14 (two rows of ducts with 4 ducts of 4 mm diameter in each row), which impart rotation to the liquid. The stream exits the swirl chamber 12 through the nozzle 15 with diameter of 12 mm, which is located in a separate bushing installed in the chamber on a thread.

On the opposite end of the body, the swirl chamber 13 is installed with the outlet nozzle 16 having diameter of 16 mm. Tangential ducts 17 of this chamber (4 ducts with diameter of 5 mm) connect it with the reservoir, to which air is supplied through the nosepiece 10. The outlet nozzles 15 and 16 of the swirl chamber are located in the chamber 18 of the body, which is connected to the discharge by the nosepiece 19. Note that tangential ducts 14 and 17 of the swirl chambers impart opposing directions of rotation to the stream, and the swirl chamber 13 imparts a higher rotation velocity to

the flow in the outlet nozzle than the swirl chamber 12. The ratio between the tangential and axial velocities in the outlet nozzles of the swirl chambers is determined by the geometrical characteristic A [15]:

$$\mathrm{A} = \frac{Rr_n}{nr_{in}^2},$$

where R is the distance from the axis of the tangential ducts in the swirl chamber; r_n is the radius of the outlet nozzle; r_{in} is the radius of the tangential duct; n is the number of tangential ducts.

According to the adopted geometry, the geometric characteristic of the swirl chamber 12 is A = 2.6, that of the swirl chamber 13 is A = 4.5.

The testing results of the above-described arrangements were compared with the test data for a conventional bubble diffuse aeration system with the diameter of the pore about 0.2 mm. A device of the ceramic disperser type for creating air bubbles was installed instead of the swirl chamber 13 (not shown in Fig. 1). The water supply location was unchanged. The air supply nosepieces 9 and 10 were plugged; the swirl chambers 12 and 13 were dismounted.

In order to study the efficiency of water-air interaction in the developed device at different arrangements, the tests were conducted with water supply to the nozzle 7 and air supply to: (a) the nosepiece 9; (b) the nosepiece 10; (c) the ceramic disperser nosepiece. In all cases the resulting two-phase stream was discharged through the nosepiece 19.

In tests with air supply to the nosepiece 9 the air stream achieves high velocity within the bushing 2 shaped as a Ventury tube. The maximal air velocity value is reached at the entrance to the throat 4 where the water is injected. The strong difference between the air and water velocities yields high quality of water atomization. Hydraulic tests of the device in this arrangement have shown that water drops in this case had diameters about 0.1-0.15 mm under low air supply pressures (2-3 bar) [14].

In tests with air supply to the nosepiece 10, the nosepiece 9 was plugged. The ducts 17 of the swirl chamber 13 imparted rotation to the air stream, which entered the chamber 18 through the nozzle 16 with tangential velocity. The water supplied to the nozzle 7 entered tangential ducts 14 of the swirl chamber 12 and exited through its nozzle 15 with oppositely directed tangential velocity. Then the water entered into the same chamber 18, where it interacted with the air stream. Interaction of the liquid and air streams rotating in opposite directions produced intense turbulence in the chamber 18 and resulted in effective saturation of water by air oxygen.

The layout of the test section is shown in Fig. 2. In all tests the air was supplied to the nosepieces 2, 3 and 4 through the respective taps by the compressor 5 producing up to 800 l/hr. The air pressure varied within the 0.2-1.2 bar range depending on the flow rate. To measure the latter, the rotameter 1 was installed on the air pipeline. Water from the tank 6 was supplied by the pump 7 to the nozzle of device 11 through the regulated faucet 8 and the rotameter 9. The pump provided for water flow rate of up to 1200 l/hr. The aerated water filled glass tank 12 with the volume of 10 l. The air bubbles in the aerated water were photographed by the optical system 10. Each set of experiments was digitally photographed 10 times at close range with exposure time 1/1000 sec to prevent blur of bubbles. All the photos were taken under the same conditions. To determine the air oxygen content in the water the OXI-340 device was used (unit 13 in Fig. 2). After finishing the test the water was discharged through the faucet 14.

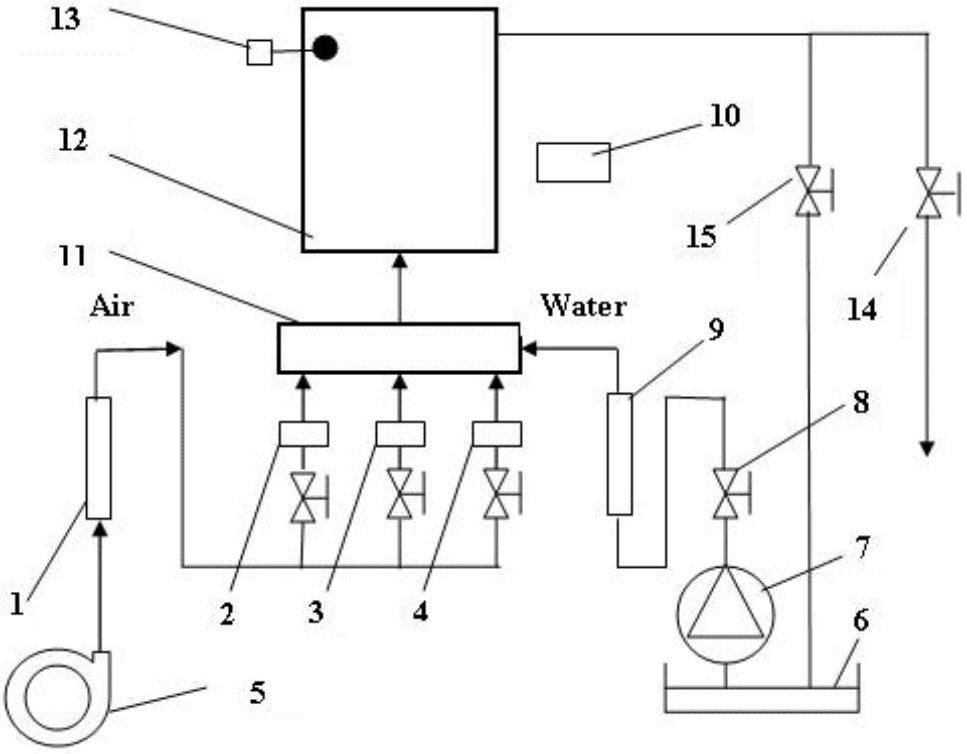

Figure 2: Test section layout.

3 Experimental program and results

The tests were conducted with tap water for each of the above-described versions of the setup arrangement. The water temperature in all the experiments was within 20 ˚-22 ˚ C. The air flow rate was constant at 250 l/hr; the water flow rate was changed within the 2-20 l/hr range. The water supply pressure varied within the 0.05-3 bar range. The data obtained were used to find the water flow rate at which the finest bubbles were generated (Fig. 3).

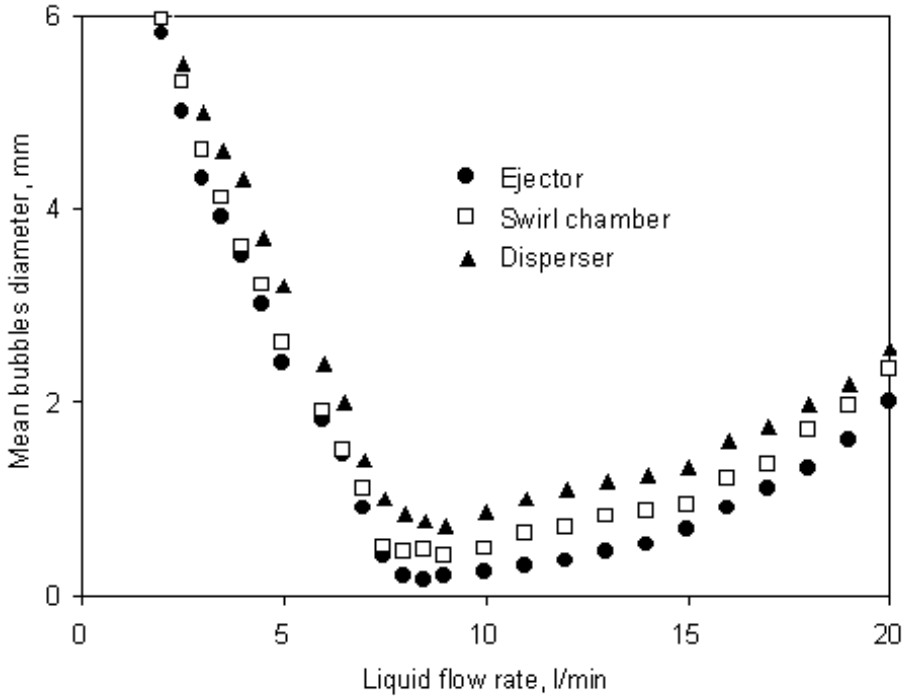

Figure 3: Air bubble diameters at variable water and constant air flow rates.

Every image of aerated water in a glass tank was processed with MATLAB program, which identified the borders of bubbles and estimated their mean diameter. In the case of adjoining bubbles their size and number were estimated using watershed transform, which is widely used in image processing for segmentation of contiguous objects. Then the actual size of the bubbles and their distribution were calculated. In further tests the water flow rate kept constant while the air flow rate varied within the range of

50-800 l/hr in order to study the influence of the air/water flow rates ratio on the bubbles size (Fig. 4).

The air oxygen content in the water was measured by the OXI-340 device. The samples for measurements were taken from the tank 12 (Fig. 2) every minute. In the tests the water was discharged from this tank through the faucet 15 into the tank 6, from where the aerated water was returned to the device through the pump. The water flow rate was 10 l/hr, the air flow rate 500 l/hr. Thus the water in the tank 12 (Fig. 2) was fully replaced within a minute. After the preset oxygen content in water was reached, the air and water supply to the device was stopped and the decrease in the oxygen content with time was monitored (Figs. 5 and 6).

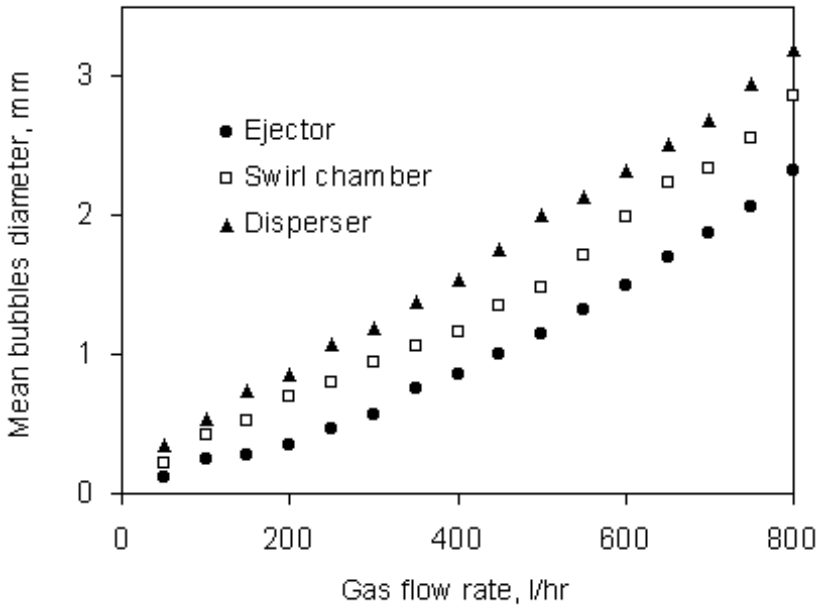

Figure 4: Air bubble diameters at constant water and variable air flow rates.

It follows from Fig. 3 that in the entire range of water flow rates the smallest air bubbles were produced when ejector was used, and the largest ones with ceramic disperser. For instance, at water flow rate of 4.5 l/min (the ratio between the air and water flow rates $k = m_a/m_w = 1.08$), the mean air bubble diameters were 3 mm, 3.2 mm and 3.7 mm for ejector water supply, swirl chamber, and ceramic disperser, respectively. At water flow

rate of 20 l/min the respective bubble diameters were 2 mm, 2.3 mm, and 2.6 mm. The finest bubbles were produced in the flow rate range of 8-10 l/min. The minimal values of the mean bubble diameter were achieved at the flow rate of 8.5 l/min ($k = 0.49$) and were equal to 0.15 mm, 0.46 mm, and 0.77 mm, respectively.

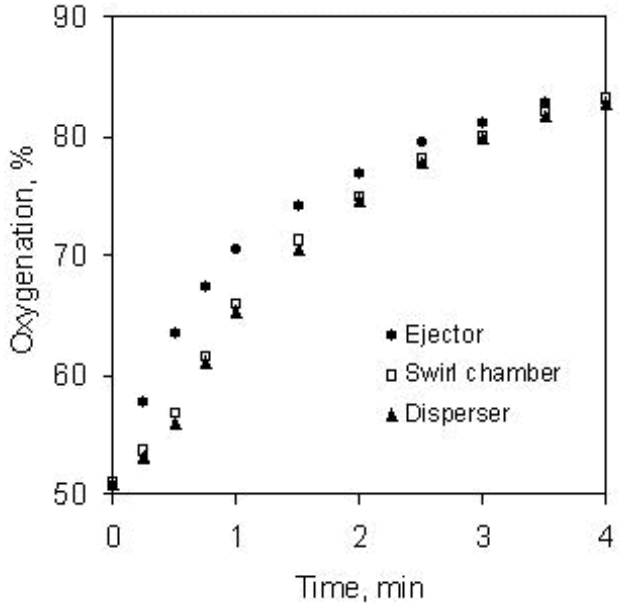

Figure 5: Oxygen content in water as a function of aeration duration.

It can also be seen from experimental curves in Fig. 3 that in the range of small water flow rates (before the minimal bubble diameter is achieved) the influence of the ratio k on the air bubble diameter size is stronger than at large water flow rates. At the water flow rate of 7 l/min the mean bubble diameters were equal to 0.9 mm, 1.1 mm, and 1.4 mm respectively, while at the 7.5 l/min flow rate they decreased to 0.4 mm, 0.5 mm, and 1 mm, respectively. The observations have shown that after the minimum on the curves on the Fig. 3 has been passed, the mean bubble size grew with air flow rate. The growth in bubble mean diameter after its minimum was reached (Fig. 3) with further increase in air flow rate can be explained by insufficiency of the water flow rate for creation small bubbles in the water. Note that in the water flow range below the minimum point, the experimental data for ejector and swirl chamber tests are close, while outside

this region the difference between bubble sizes obtained in these two test series increases.

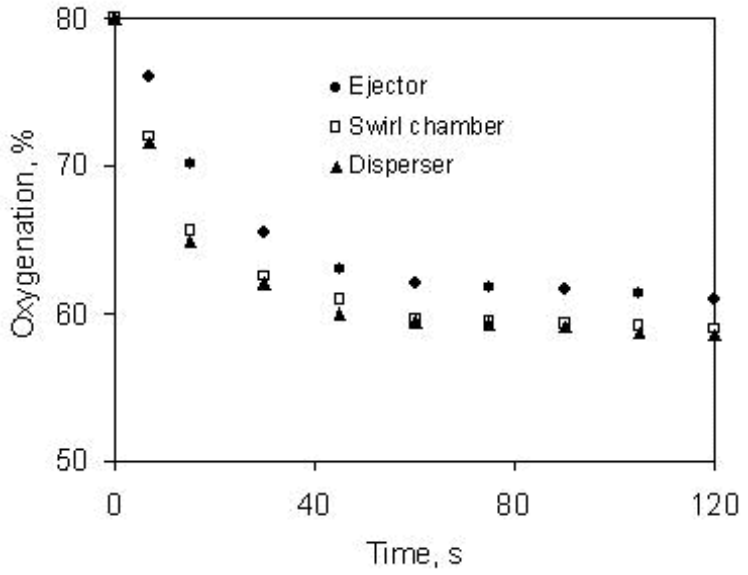

Figure 6: Reduction of the oxygen content in water after termination of aeration.

The influence of the parameter k on the air bubble sizes was studied at a constant water flow rate $m_w = 11$ l/min and variable air flow rate m_a (Fig. 4). According to previous results, it was found that increase in k beyond its value corresponding to the minimal bubble size yields generation of larger bubbles. Their size increases monotonically with k (see Fig. 4), and the smallest bubbles were obtained in the ejector tests, while the largest ones with the conventional arrangement.

The rate of water saturation by air oxygen in different test conditions is presented in Fig. 5. The starting point for all measurements corresponds to the oxygen content in tap water. With increase of the test duration, resulting in longer air/water interaction within the device, the oxygen content in the water rises. Regardless of the specific disperser kind used in the tests, after about 2 minutes of aeration the percent of oxygenation is practically unchanged in time. The highest rate of water oxygenation is registered during the first minute of aeration. Note that the best result was obtained in the ejector tests, while the least rate of oxygenation was in the case of

ceramic disperser. Thus, by the end of the first minute of the tests the oxygen content in the water was 70.5%, 66%, and 65%, respectively. To reach the same value of oxygen content in water which was obtained with the use of ejector to this time moment, in the disperser-based device 50% more time was needed. As the aeration duration increases, the oxygen content in water approaches the same value regardless of the device arrangement. After 3 minutes of tests the oxygen content in water was 81% in the ejector tests and 80% in the cases of swirl chamber and ceramic disperser.

After termination of aeration the solute oxygen gradually left the water; the process is characterized by the data in Fig. 6. It follows from the test results that the rate of oxygen removal is the least in the case of ejector based aerator. In both other cases (swirl chamber and ceramic dispenser) the rate of the oxygen removal was approximately the same. Note that the oxygen content in water by the end of monitoring remains higher in the case of ejector-based aerator (62% as against 58%).

4 Conclusions

1. The ejector and swirl chamber based aerators produce smaller bubbles than aerators using ceramic dispersers under similar conditions of air/water interaction.

2. Experimental data indicate that dependence of the bubbles sizes on the water/air flow rates ratio has a minimum.

3. Increase in the air flow rate after the minimal bubble size is reached yields an increase in the bubbles sizes.

4. The most efficient water oxygenation was achieved in an ejector-based aerator.

5. After the aeration is terminated the oxygen content remains higher in the case of ejector-based device.

6. There exists a certain minimal air flow rate providing the most efficient water saturation with air oxygen at a preset water discharge in an aerator.

References

[1] H.J. Hwang and M.K. Stenstrom, J. Water Pollution Control Federation **57**, 12 (1985).

[2] T. Jones, J. Water & Wastewater **18**, 6 (2003).

[3] *Encyclopedia of Aquaculture*, Ed.: R.R. Stickney (World Aquaculture Society, USA, 2000).

[4] G.L. Huibregtse, T.C. Rooney, and D.C. Rasmussen, J. Water Pollution Control Federation **55**, 657 (1983).

[5] M.N. Hedaoo and A.G. Bhole, 26th WEDC Conference, p. 274 (Dhaka, Bangladesh, 2000).

[6] M.K. Stenstrom and R.G. Gilbert, Water Research **15**, 6 (1981).

[7] Y. Sheng-Ping, J. Ind. and Eng. Chem. Res. **42**, 25 (2003).

[8] K.I. Ashley, K.J. Hall, and D.S. Mavinic, Water Research **25**, 12 (1991).

[9] D. Guilbert, R. Ben Aim, H. Rabie, and P. Cote, J. Desalination **148**, 395 (2002).

[10] M. Wagner and H.J. Popel, J. Water Science Technology **34**, 249 (1996).

[11] J.M. Chern, S.R. Chou, and C.S. Shang, Water Research **35**, 13 (2001).

[12] V.L. Burris, D.F. McGinnis, and J.C. Little, Water Research **36**, 4605 (2002).

[13] C.D. DeMoyer, E.L. Schierholz, J.S. Gulliver, and S.C. Wilhelms, Water Research **37**, 1890 (2003).

[14] M.P. Levitsky, Y.M. Shtemler, and Y. Berkovich, International Symposium on Multiphase Flow and Transport Phenomena, p. 497 (Antalya, Turkey, November 5-10, 2000).

[15] G.N. Abramovich, *Applied Gas Dynamics* (Nauka, Moscow, 1991).